CrossMark

Wind effects on 'Z' plan-shaped tall building: a case study

Rajdip Paul[1] · Sujit Kumar Dalui[1]

Abstract The present paper is centered on the study to understand the behavior of various surfaces of a 'Z' plan-shaped tall building under varying wind directions. For that purpose, computational fluid dynamics (CFD) package of ANSYS is used. The length scale is considered as 1:300. Force coefficients both in the along and across wind direction as well as the external surface pressure coefficients for different faces of the object building are determined and listed for wind incidence angle 0°–150° with increment of 30°. The wind flow pattern around the building showing flow separation characteristics and vortices are presented. The variation of wind pressure on different surfaces of the building is clearly shown by contour plots. The nature of deviation of external pressure coefficients along the height of the building as well as along the perimeter of the building for different wind angles of attack is presented. The force coefficient (C_f) along the X direction is extreme for 15° wind angle and along Y direction it is maximum for 60° angle of attack. Unsteady vortices are generated in the wake region due to a combination of positive and negative pressure in the windward and leeward faces, respectively.

✉ Sujit Kumar Dalui
sujit_dalui@rediffmail.com

Rajdip Paul
rajdippaul87@gmail.com

[1] Department of Civil Engineering, Indian Institute of Engineering Science and Technology, Shibpur, Howrah, India

Introduction

As buildings are cantilever structures, there is generation of base moment whenever it is under lateral load. The magnitude of the moment increases considerably with slenderness, because the moment is proportional to the square of the height of the building, just like a cantilever beam under varying loads. Because of the scarcity of land these days, vertical construction is given due importance and the buildings are much higher than before, making them highly susceptible to horizontal loading like wind load. In addition to this, if the plan of the building is unconventional, then wind analysis is a task of great complexity because of the many flow situations arising from the interaction of the wind with the structures. There are several different phenomena giving rise to dynamic response of tall structures under wind such as buffeting, vortex shedding, galloping and flutter. Simple quasi-static analysis of wind loading, which is globally applied to the design of low- to medium-rise structures, can be unacceptably conservative for the design of very tall buildings. At present, the wind tunnel model experiment and numerical simulation using computational fluid dynamics (CFD) are the available research tools to get deeper insight into the behavior of gigantic structures subjected to turbulent wind load.

In the definition of the overall strength, durability and risk of failure of structures, extreme wind speed is an important factor, mostly reliant on the general weather pattern over many years and local environmental and topographical conditions.

The precise evaluation of the extreme wind is mainly connected with the quality of statistical data of wind velocity which is associated with performance and calibration of measuring instruments, common averaging time, same height above the ground, roughness of the terrain, etc.
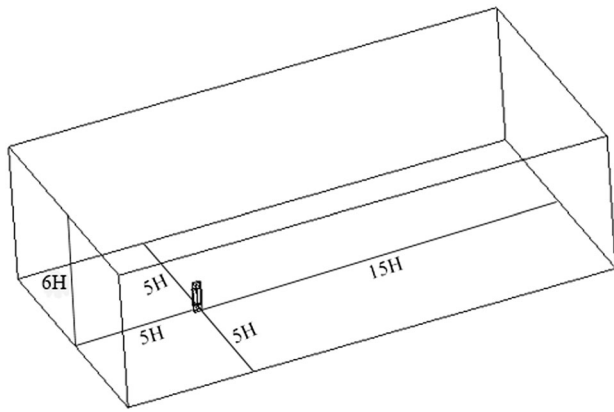
Springer

Fig. 1 Domain used for the study

The predicted wind speed is usually enumerated as the maximum wind speed which is surpassed, on average, once in every N year (return periods); for example, I.S: 875 (Part-3) (1987) requires that ordinary structures be designed for an annual exceed probability of 2 % which is equivalent to 50 years of return periods.

Past studies have been carried out by researchers with the help of model analysis to get more accurate information regarding wind structure interaction. Kareem (1986) deliberated the details of the interference and proximity effects on the dynamic response of prismatic bluff bodies. Lin et al. (2004) discussed the findings of a widespread wind tunnel study on local wind forces on isolated tall buildings based on the experimental outcome of nine square and rectangular models (1:500). Liang et al. (2004) proposed the empirical formulae for different wind-in-duced dynamic torsional responses through the analytical model. Gomes et al. (2005) enumerated the results from the studies of L- and U-shaped models of 1:100 scale. Lam and Zhao (2006) examined in detail wind flow around a row of three square-plan tall buildings closely arranged in a row at a wind angle $\theta = 30°$. The computational domain was

digitized into 2.1×10^6 finite volumes. Irwin (2007) reviewed a number of bluff body aerodynamic phenomena and their effect on the structural safety and occupant comfort. Zhang and Gu (2008) correlated the numerical
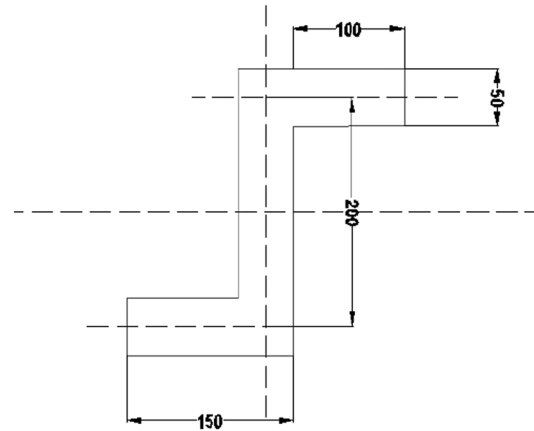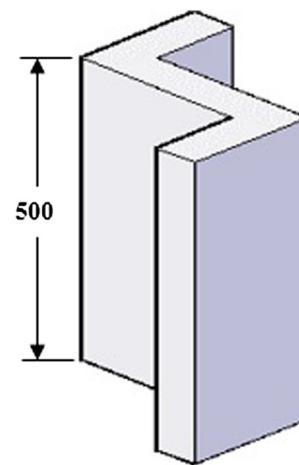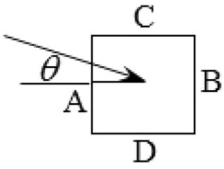

Fig. 2 Plan of 'Z' plan-shaped building model

Fig. 3 Isometric view of the model

Table 1 Surface pressure coefficients for a square building

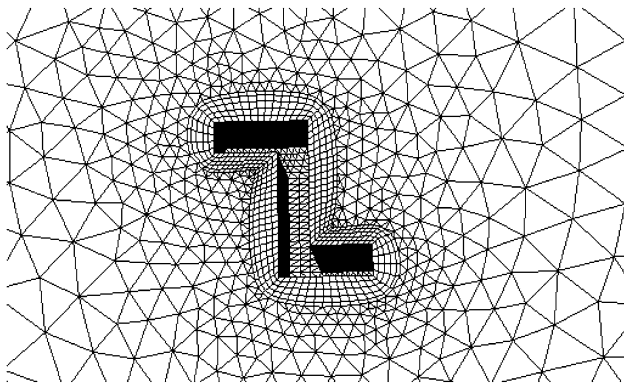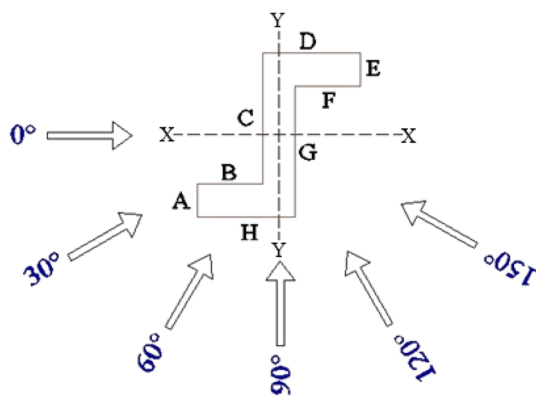| Plan of the building	As per	$\dfrac{h}{w}$	Wind angle (θ) (°)	C_{pe} for surfaces			
				A	B	C	D
	ANSYS CFX	$\dfrac{h}{w} = 5$	0	+0.80	−0.40	−0.60	−0.60
			90	−0.60	−0.60	+0.80	−0.40
	AS-NZS 1170-2:2002	Any $\dfrac{h}{w}$	0	+0.80	−0.50	−0.65	−0.65
			90	−0.65	−0.65	+0.80	−0.50
	ASCE 7-10	Any $\dfrac{h}{w}$	0	+0.80	−0.50	−0.70	−0.70
			90	−0.70	−0.70	+0.80	−0.50
	I.S: 875 (Part-3) (1987)	$\dfrac{3}{2} < \dfrac{h}{w} < 6$	0	+0.80	−0.25	−0.80	−0.80
			90	−0.80	−0.80	+0.80	−0.25

Fig. 4 Mesh pattern around the building

Fig. 5 Name of the different faces of the building

simulation and experimental investigations of wind-induced interference effects. Fu et al. (2008) enumerated the field measurements of the characteristics of the boundary layer and storm response of two super tall buildings. Irwin (2009) centered on the subject of determining and controlling the structural response under wind action for super tall buildings which demand much more pragmatically modeled wind engineering, since building codes and standards are not practical enough for dealing with such soaring structures. Tse et al. (2009) discussed the general concept to determine the wind loadings and wind-induced responses of square tall buildings with different sizes of chamfered and recessed corners while maintaining the total usable floor area of the building by escalating the number of stories which is directly associated with the economics of the building. Bhatnagar et al. (2012) presented the results of a wind tunnel study in an open circuit boundary layer flow condition, carried out on a model of low-rise building with sawtooth roof. Tominaga and Stathopoulos (2012) modeled turbulent scalar flux in computational fluid dynamics (CFD) for near-field dispersion around buildings. Raj et al. (2013) carried out an experimental boundary layer wind tunnel study to observe the effect of base shear, base moment and twisting moment developed due to wind load on a rigid building model having the same floor area, but different cross-sectional shapes with the variation of wind incidence angle. Muehleisen and Patrizi (2013) developed parametric equations to find out the values of pressure coefficients (C_p) on the surfaces of rectangular
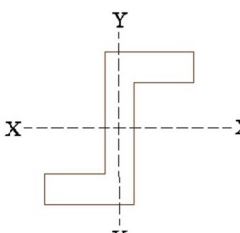
Table 2 Force coefficients for the building

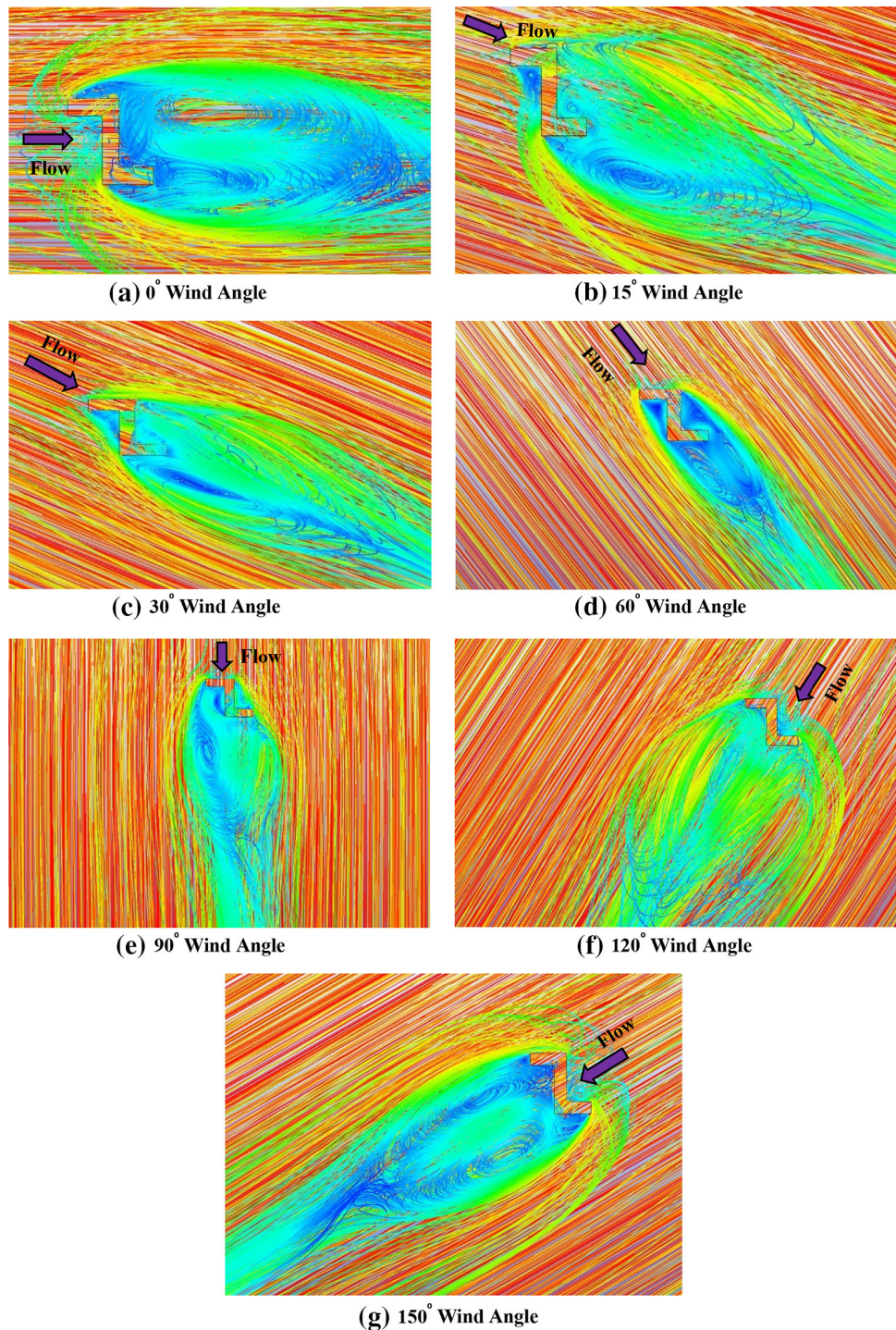| Plan of the building	Wind angle (°)	Force coefficients C_f	
		Along X	Along Y
	0	+0.96	+0.01 $\approx$ 0
	15	+1.02	+0.29
	30	+0.88	+0.52
	60	+0.73	+1.24
	90	+0.01 $\approx$ 0	+1.04
	120	−0.35	+0.62
	150	−0.61	+0.35

Table 3 Surface pressure coefficients for the building

Wind angle (°)	C_{pe} (face average value) for different faces of the building							
	Face A	Face B	Face C	Face D	Face E	Face F	Face G	Face H
0	0.74	0.84	0.73	−0.58	−0.41	−0.47	−0.46	−0.62
15	0.69	0.66	0.61	−0.66	−0.54	−0.52	−0.45	−0.50
30	0.73	0.29	0.36	−0.50	−0.46	−0.50	−0.44	0.06
60	−0.50	−0.55	−0.42	−0.30	−0.37	−0.48	−0.50	0.50
90	−0.64	−0.47	−0.52	−0.43	−0.61	0.06	−0.18	0.69
120	−0.57	−0.38	−0.49	−0.48	−0.64	0.74	0.81	0.53
150	−0.54	−0.41	−0.43	−0.69	−0.21	0.87	0.86	−0.37

low-rise building models from experimental wind tunnel data. Amin and Ahuja (2013) investigated through wind tunnel studies rectangular building models of different side ratios (ratio of building's depth to width) ranging from 0.25 to 4, keeping the area and height the same for all models, while the wind angle changes at an interval of 15° from 0° to 90°. Kushal et al. (2013) recognized that the plan shape of the building affects the wind pressure to a great degree.

Verma et al. (2013) described the effects of wind incidence angle on wind pressure distribution on square-plan tall buildings. Bhattacharyya et al. (2014) investigated the mean pressure distribution on various faces of 'E' plan-shaped tall building through experimental and analytical studies for a wide range of wind incidence angle. Chakraborty et al. (2014) enumerated the results of a wind tunnel study and numerical studies on '+' plan-shaped tall

Fig. 6 Wind flow pattern around the building for various wind angles

(a) 0° Wind Angle

(b) 15° Wind Angle

(c) 30° Wind Angle

(d) 60° Wind Angle

(e) 90° Wind Angle

(f) 120° Wind Angle

(g) 150° Wind Angle

building and compared the results for 0° and 45° wind incidence angles. Kheyari and Dalui (2015) have conferred the results of a case study to estimate wind load on a tall building under interference effects. They used a CFD simulation tool to create a 'virtual' wind tunnel to predict the wind characteristics and wind response.

Mean wind speed profiles

Wind velocity is thought to be zero at ground, and persistently intensifying the mean wind speed with height can be presented by two models: to be specific, logarithmic law and power law. At some height, the air movement is thought to be free from the Earth's frictional resistance.

Height fluctuates for distinctive terrain category. The dissimilarity in temperature offers rise to the gradients of pressure which set air in motion.

1. Logarithmic law:

$$\frac{V_z}{V^*} = \frac{1}{k} \log_e \frac{z}{z_0},$$ (1)

where k is the Von Karman's constant $= 0.40$, z the height above the ground, z_0 the surface roughness parameter, V_* the friction viscosity $= \sqrt{\frac{\tau_0}{\rho}}$, τ_0 the skin frictional force on the wall and ρ the density of air.

2. Power law:

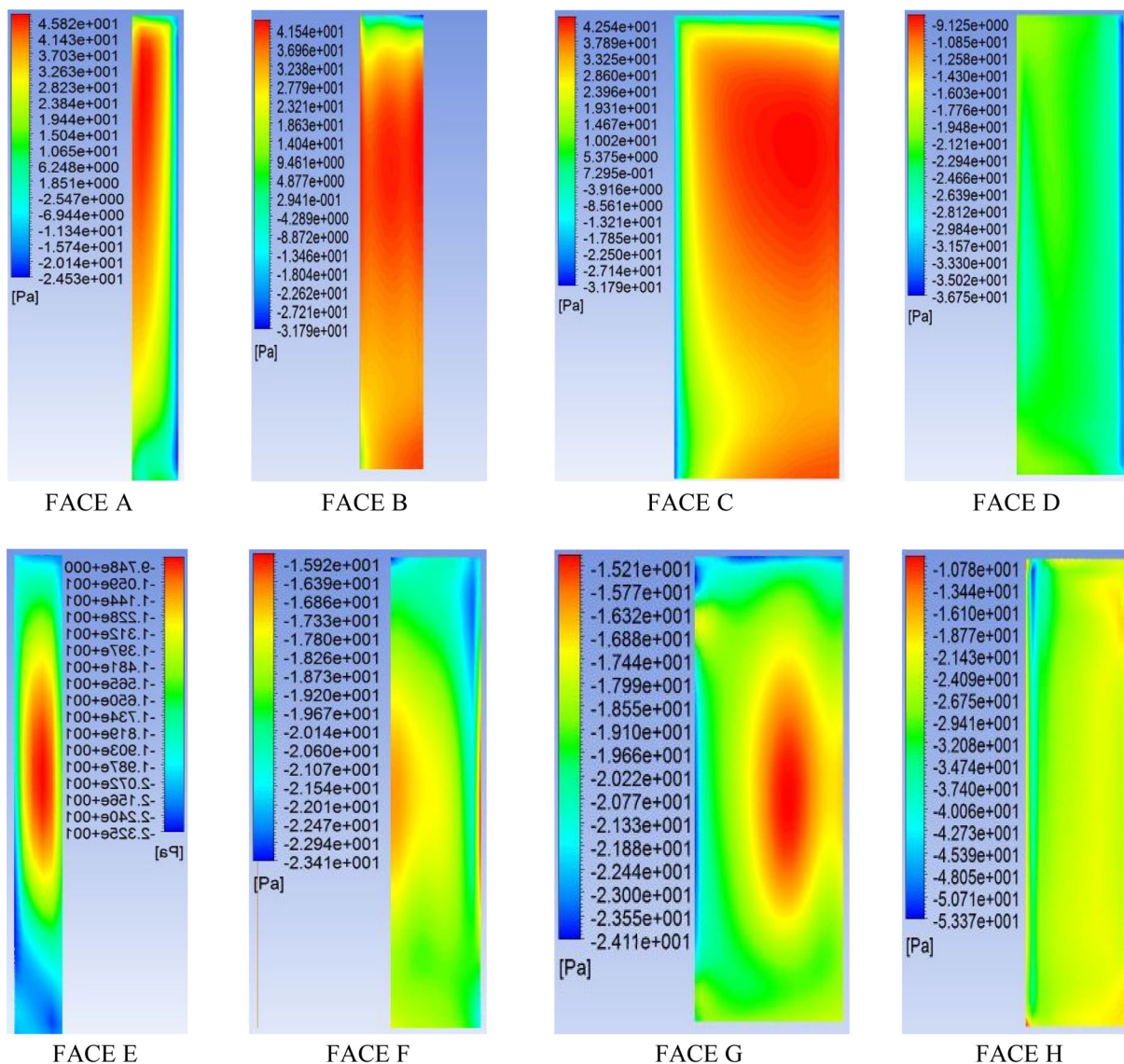$$\frac{V}{V_0} = \left(\frac{z}{z_0}\right)^{\alpha},$$ (2)

Fig. 7 Variation of wind pressure on different surfaces of the building for a wind incidence angle of 0°

where, V is the velocity at height z above the ground, V_0 the wind speed at reference height, z_0 the reference height above the ground, generally 10 m, and α the exponent power law, varying for different terrains.

Among these two, the power law is widely used by researchers as it is quite easy to adjust match with mean wind velocity profile.

Computational fluid dynamics (CFD)

Computational fluid dynamics is a computer simulation tool that creates a 'virtual' wind tunnel to envisage the motion of fluids around objects. By virtue of advancements in high speed computing and parallel processing, the CFD technique is a powerful augmentation of the physical wind tunnel, which together enables us to solve complex wind flow problems. CFD is a versatile and powerful tool that can be used to solve problems related to pedestrian-level wind comfort, cladding pressures on buildings, etc.

There are several methods in CFD to foresee the wind flow and their effects. Here, ANSYS CFX, AN-SYS 14.5. ANSYS. Inc. software will be used with k–ε turbulence modeling, so that decent resemblance is maintained between the experimental and numerical techniques. Gradient diffusion hypothesis is used in the k–ε model to relate the Reynolds stresses to the mean velocity gradients and turbulence viscosity. 'k' is the turbulence kinetic energy defined as the variance of fluctuations in velocity and 'ε' is the turbulence eddies dissipation (the rate at which the velocity fluctuation dissipates).
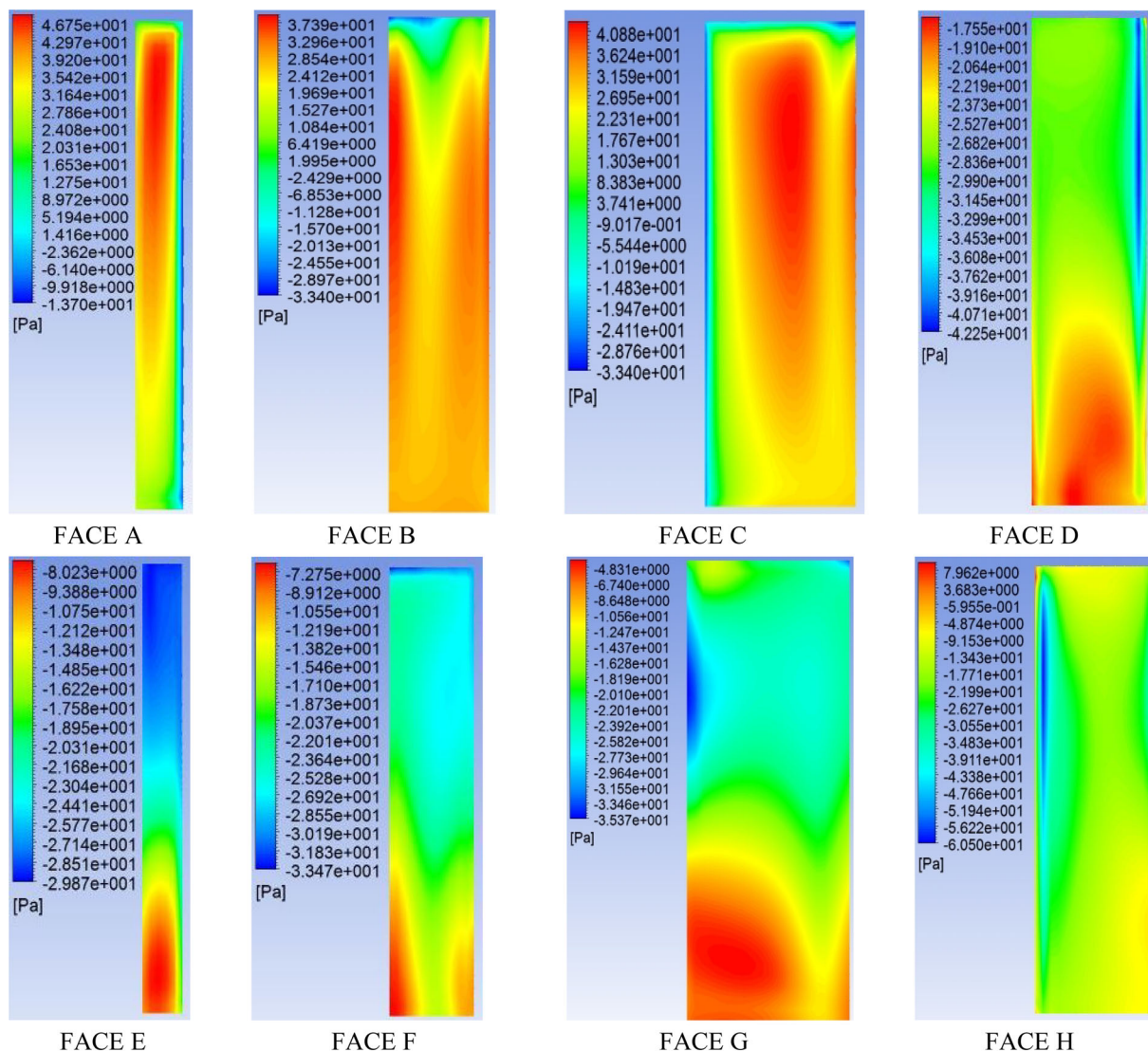

Fig. 8 Variation of wind pressure on different surfaces of the building for a wind incidence angle of 15°

Domain size shall be suitably chosen, so that vortex generation, velocity fluctuations, etc. in the wake region are effectively conformed. Revuz et al. (2012) suggested that inlet, outlet, two side face and top clearances of the domain be 5H, 15H, 5H and 5H, respectively, from the edges of the buildings, where 'H' is the height of the building. The domain is shown in Fig. 1. A combination of tetrahedron meshing and hexagonal meshing shall be considered for meshing the domain and the surface of the building model. Finer hexagonal meshing around and on the surfaces of the building is obtained by providing inflation, which leads to simulate uniform flow and measure the actual behavior of the responses accurately. Uniform coarser tetrahedron meshing in the rest of the domain will considerably reduce the time of analysis without significant loss of accuracy.

Validation of CFD

Validation of the CFD package has been done by analyzing a square building model using ANSYS CFX. From the available information of I.S: 875 (Part-3) (1987) for a simple square building of particular aspect ratio ($h/w = 5$), the pressure coefficients can be evaluated from the respective tables. Thereafter, numerical analysis was conducted in the ANSYS CFX software for a similar building model under comparable wind
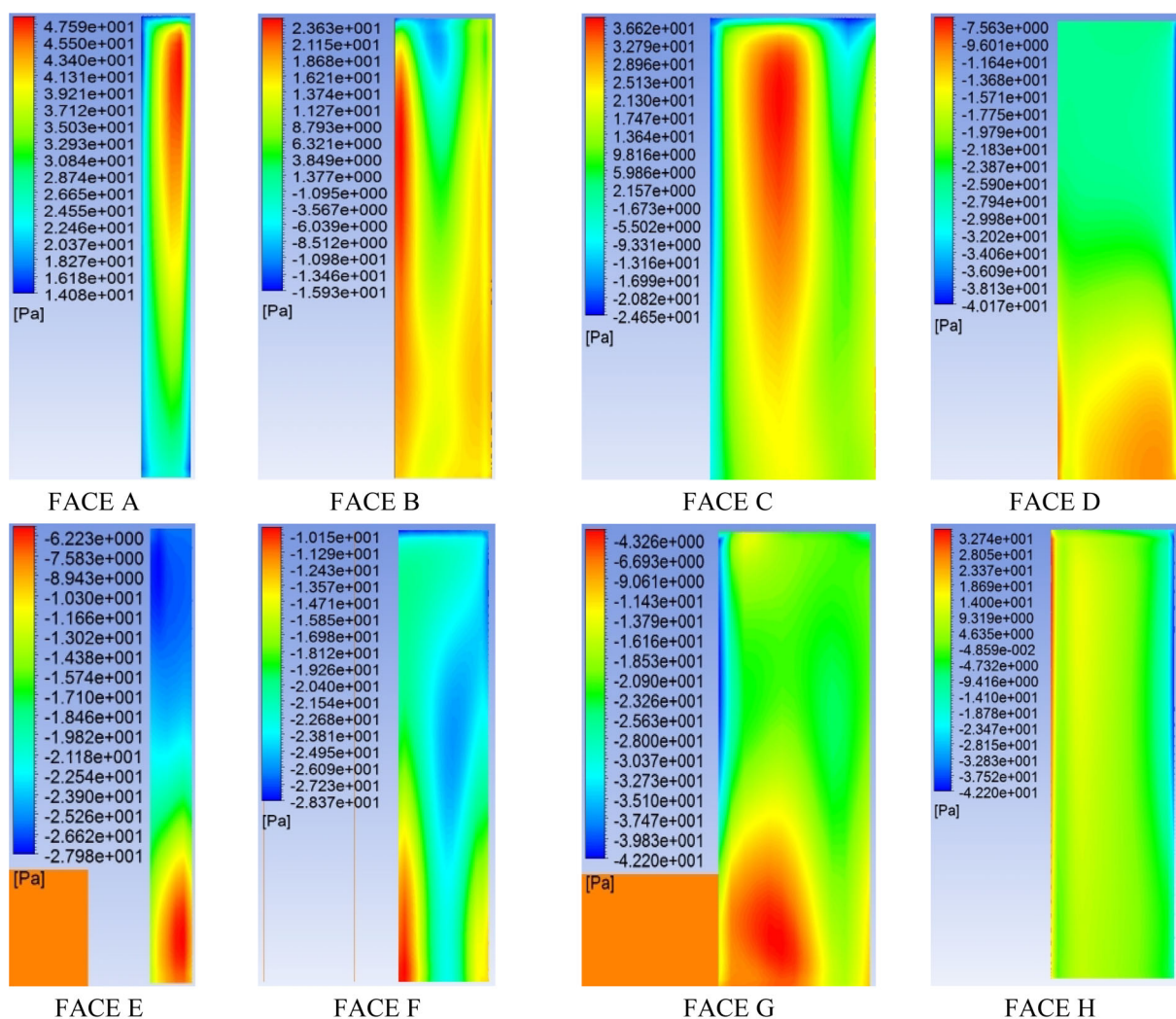

Fig. 9 Variation of wind pressure on different surfaces of the building for a wind incidence angle of 30°

environment to obtain these coefficients on different faces of the building. This evaluation obviously can be done on the basis of any other international standard of wind load.

Table 1 shows the comparison of the external pressure coefficient C_{pe} between different standards of various countries and C_{pe} calculated by ANSYS CFX for a square building. The results of the numerical analysis resembles the provisions of the code AS-NZS 1170-2:2002, Australian/New Zealand Standard, "Structural design actions, part 2: wind actions" and ASCE Standard (ASCE/SEI 7-10) "Minimum design loads for buildings and other structures", with good agreement. For the windward face, there is 0 % deviation in the result, whereas for the

sidewalls the deviation is 7.7 and 14.3 % with respect to AS-NZS 1170-2:2002 and ASCE 7-10, respectively. But for the leeward face, the result from ANSYS deviates by 20 % with respect to both the codes. This deviation in result is perhaps due to the generation of unsteady vortices in the wake region near the leeward face.

Parametric model of the study

The present study will be carried out to understand the behavior of pressure distribution on the various surfaces of a 'Z' plan-shaped building with varying wind directions. The building has clear dimensions of each limb with
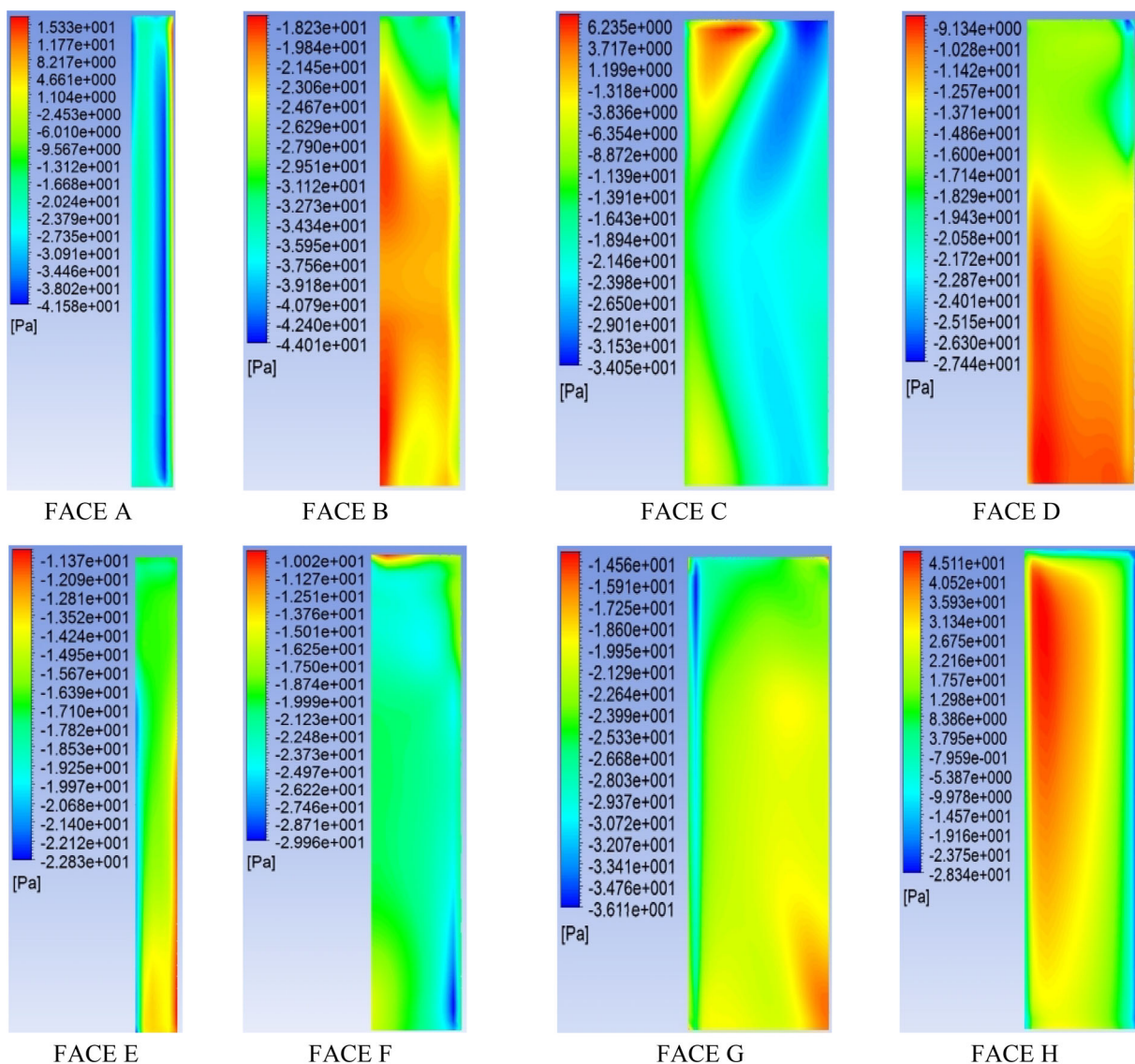

Fig. 10 Variation of wind pressure on different surfaces of the building for a wind incidence angle of 60°

100 mm length and 50 mm width (Fig. 2). The limbs are orthogonal to each other. The height of the building is considered as 500 mm. The plan area of the building is 22,500 mm^2 consequently. The rigid model length scale is considered as 1:300. The isometric view of the model is shown in Fig. 3. The domain and meshing used are as discussed in the preceding section. The mesh pattern around the building is shown in Fig. 4.

Results and discussion

The numerical study of the model as stated before has been done by the k–ε turbulence model using ANSYS CFX. The domain, meshing and flow pattern are considered as discussed earlier. Different faces are named for reference as shown in Fig. 5. The directions of the wind considered are indicated also in the same figure.

External force and pressure coefficients for the building

Force coefficients (C_f) along the X and Y direction are determined using the formula $C_f = F/(P \times A)$, where 'F' is the total force exported from numerical simulation in the desired direction corresponding to the wind angle, 'P' is the wind pressure and 'A' is the surface area exposed to the wind. Wind incidence angle 0°–150° with an interval of 30° is considered. An additional wind angle 15° is also
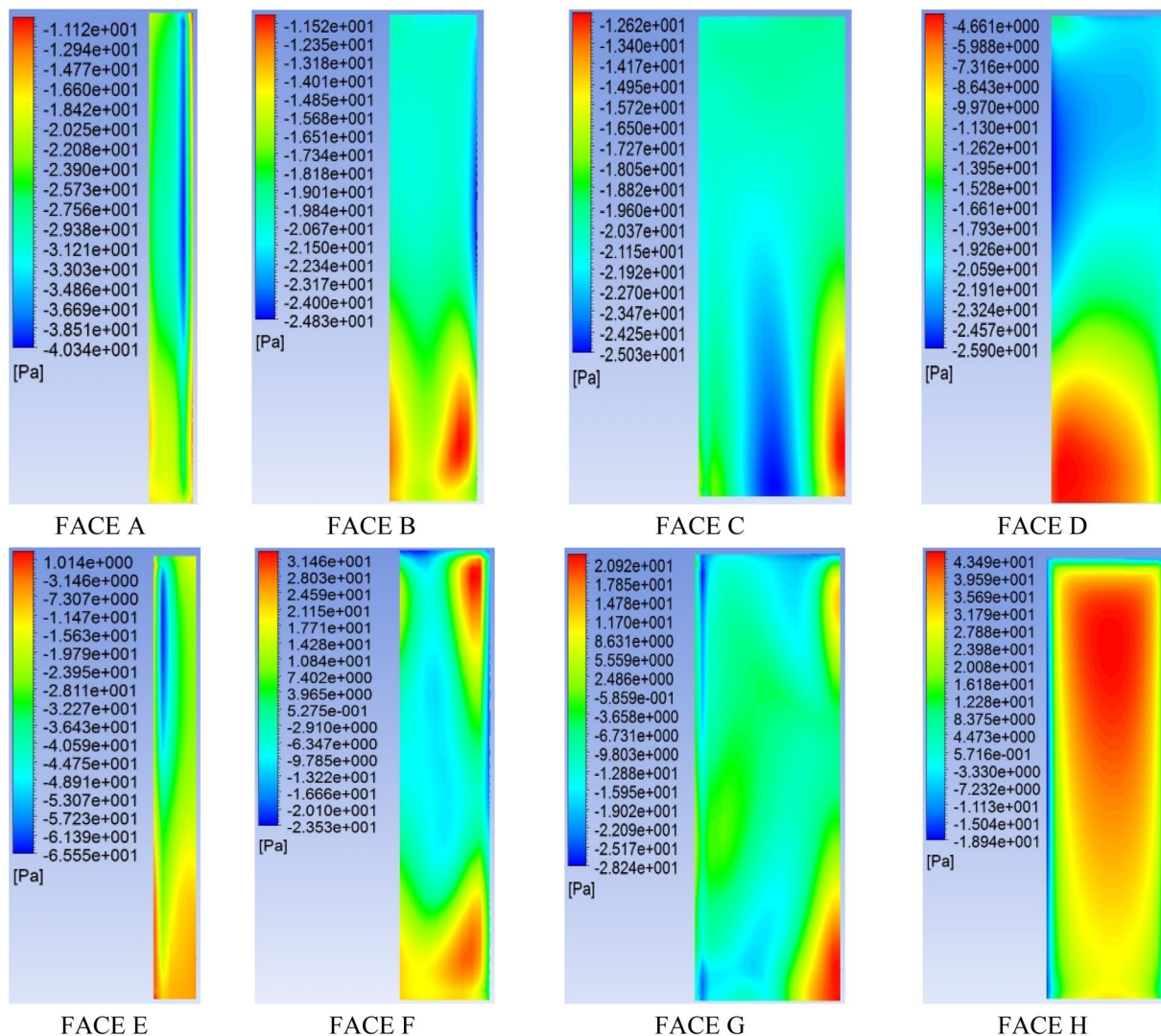

Fig. 11 Variation of wind pressure on different surfaces of the building for a wind incidence angle of 90°

considered. The coefficients are presented in Table 2. The force coefficient along the X direction is maximum for a 15° wind angle and the same along Y is maximum for a 60° wind angle of attack. A negative sign indicates suction. The wind pressure obtained by the computational method using the ANSYS CFX is used to calculate the external pressure coefficient 'C_{pe}' using the formula $C_{pe} = P/(0.6V_z^2)$, where V_z is the design wind speed and 'P' is the wind pressure. The external surface pressure coefficients, C_{pe} (face average value), for different faces of the building are listed in Table 3. Positive pressure coefficients occur at the windward faces because of direct wind dissipation and

suction pressure at the leeward faces due to frictional flow separation and vortex generation.

The wind flow pattern around the building for different wind incidence angles is shown in Fig. 6. Flow separation characteristics and vortices are quite evident from the flow patterns. The variations of wind pressure on different surfaces of the building for wind angles 0°, 15°, 30°, 60°, 90°, 120° and 150° are shown in Figs. 7, 8, 9, 10, 11, 12 and 13, respectively. Referring to Fig. 14a–g, it is quite clear that the Face A, Face B and Face C being the windward faces for wind incidence angle 0° are subjected to positive pressure, of which Face A has the lowest face average C_{pe}
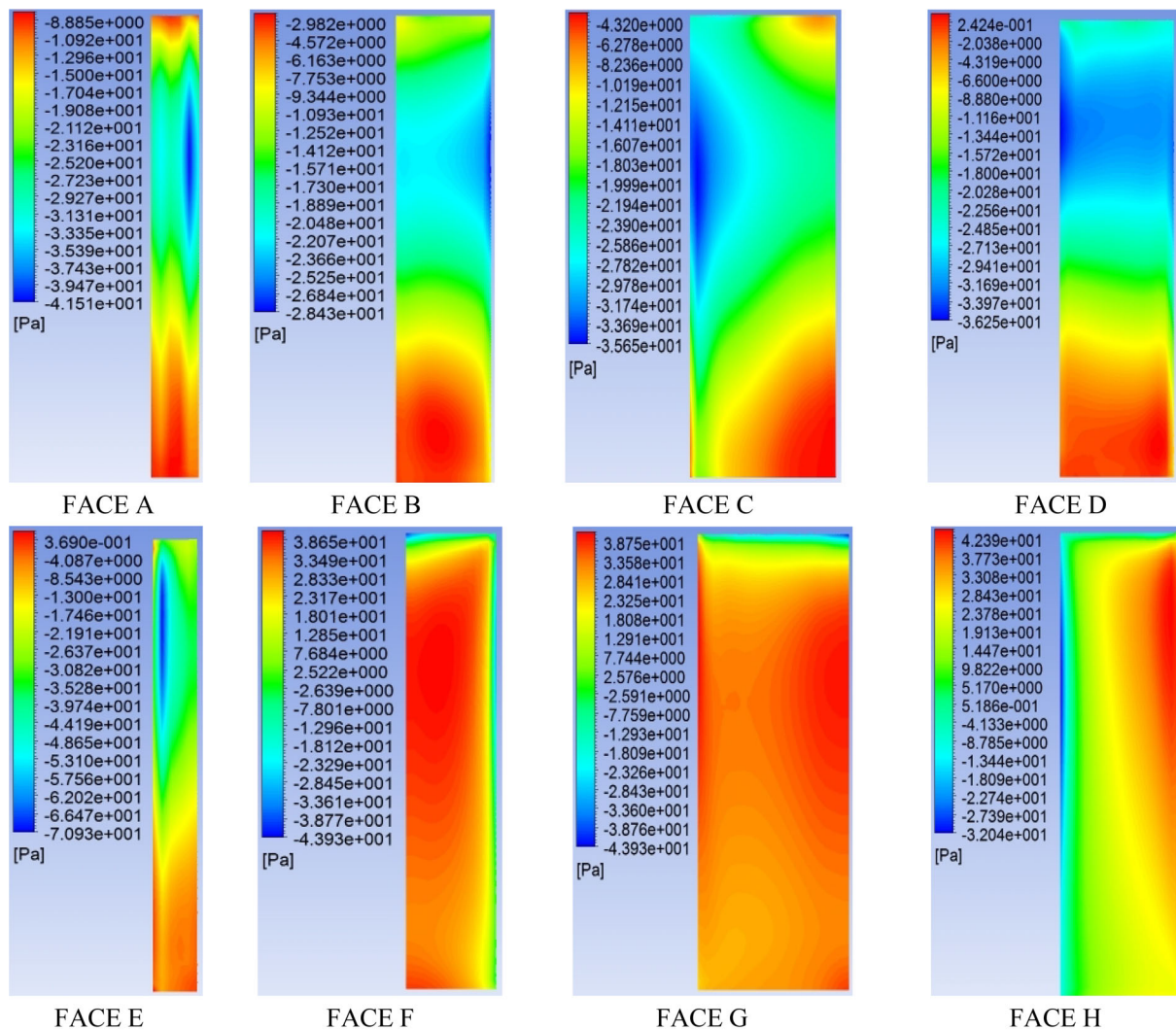

Fig. 12 Variation of wind pressure on different surfaces of the building for a wind incidence angle of 120°
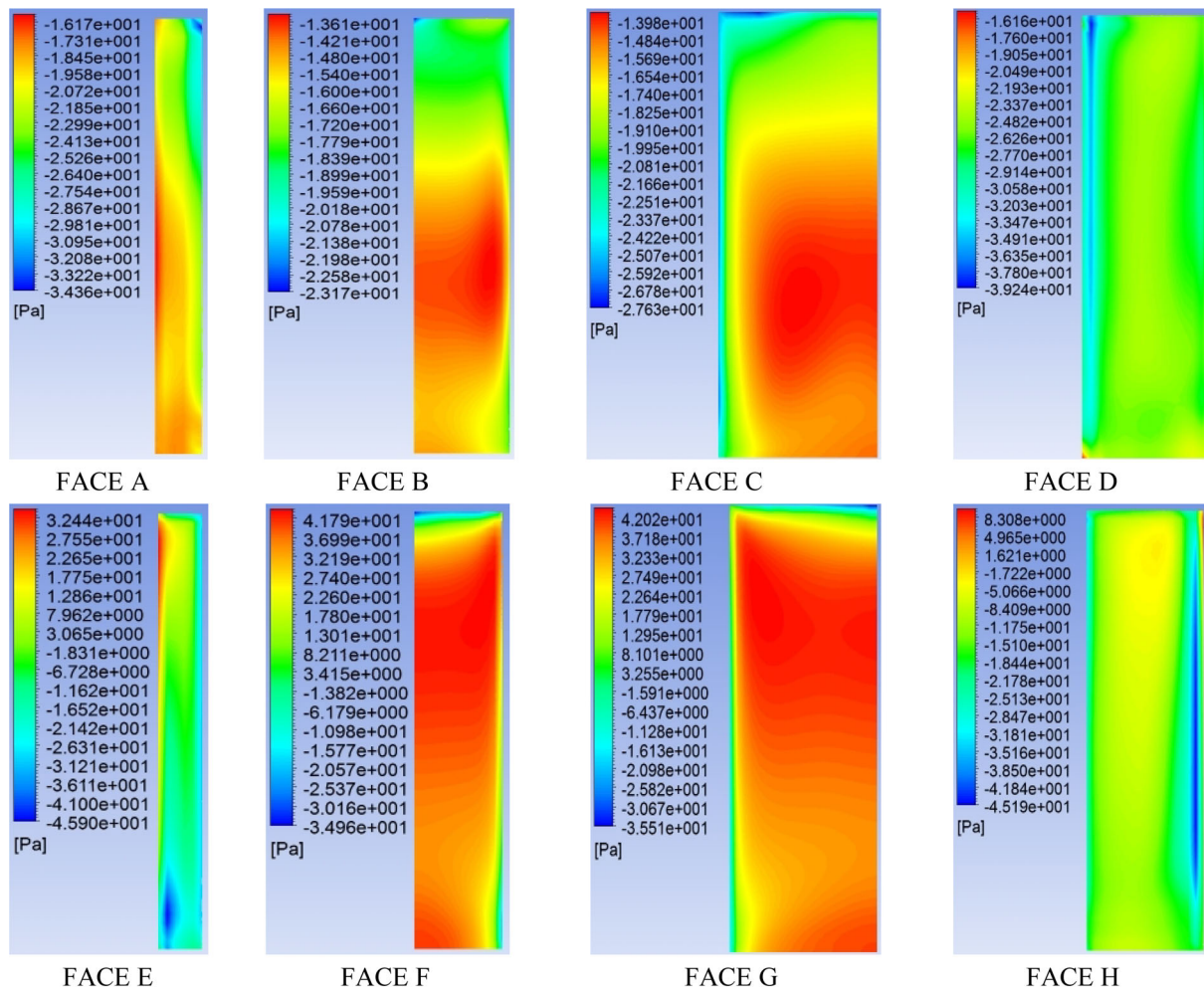
Fig. 13 Variation of wind pressure on different surfaces of the building for a wind incidence angle of 150°

because of the uplift force and backwash. Face D, Face E, Face F, Face G and Face H are exposed to suction pressure. Again, positive pressure occurs at Face A, Face B and Face C for 15° wind angle of attack. But in this case, Face A has the maximum C_{pe} at a certain height and also maximum face average C_{pe} among faces having positive pressure because of reduced backwash effect. Other faces are subjected to suction pressure again. The nature of variation of C_{pe} along the height of the building can be seen from the graph and face average values are available in Table 3. For 30° wind angle, there is positive pressure on Face B up to a certain height and then it suffers suction pressure. Face A is purely under positive pressure. The variation of C_{pe} for Face H is almost linear. The pressure is positive, but of very low (face average C_{pe} is 0.06) magnitude. When the wind incidence angle is increased to 60°, Face A, Face B and Face C, which are exposed to positive pressure up to

30° wind angle, are now changed to suction pressure. All the faces, except Face H, are subjected to negative pressure now. In case of 90° wind angle, the pressure at Face F is positive for some height and then decreases to negative. At greater height, it touches positive pressure again and ultimately suction at the top. This results in small face average C_{pe} of 0.06 for Face F. The pressure is positive for Face H and there is suction pressure for the rest of the faces. When the wind angle of attack is 120°, Face F, Face G and Face H become windward faces and are subjected to positive pressure, while the other faces are exposed to suction pressure. The maximum positive pressure occurs at Face F and the maximum negative pressure at Face E. For wind angle 150°, there is an interesting scenario of overlapping pressure variations along the height for Face F and Face G. The pressure variation is positive for both the faces and the face average C_{pe} is almost same consequently. The

Fig. 14 Variation of pressure coefficients along the vertical centerline on different faces for various wind angles

(a) 0° Wind Angle

(b) 15° Wind Angle

(c) 30° Wind Angle

(d) 60° Wind Angle
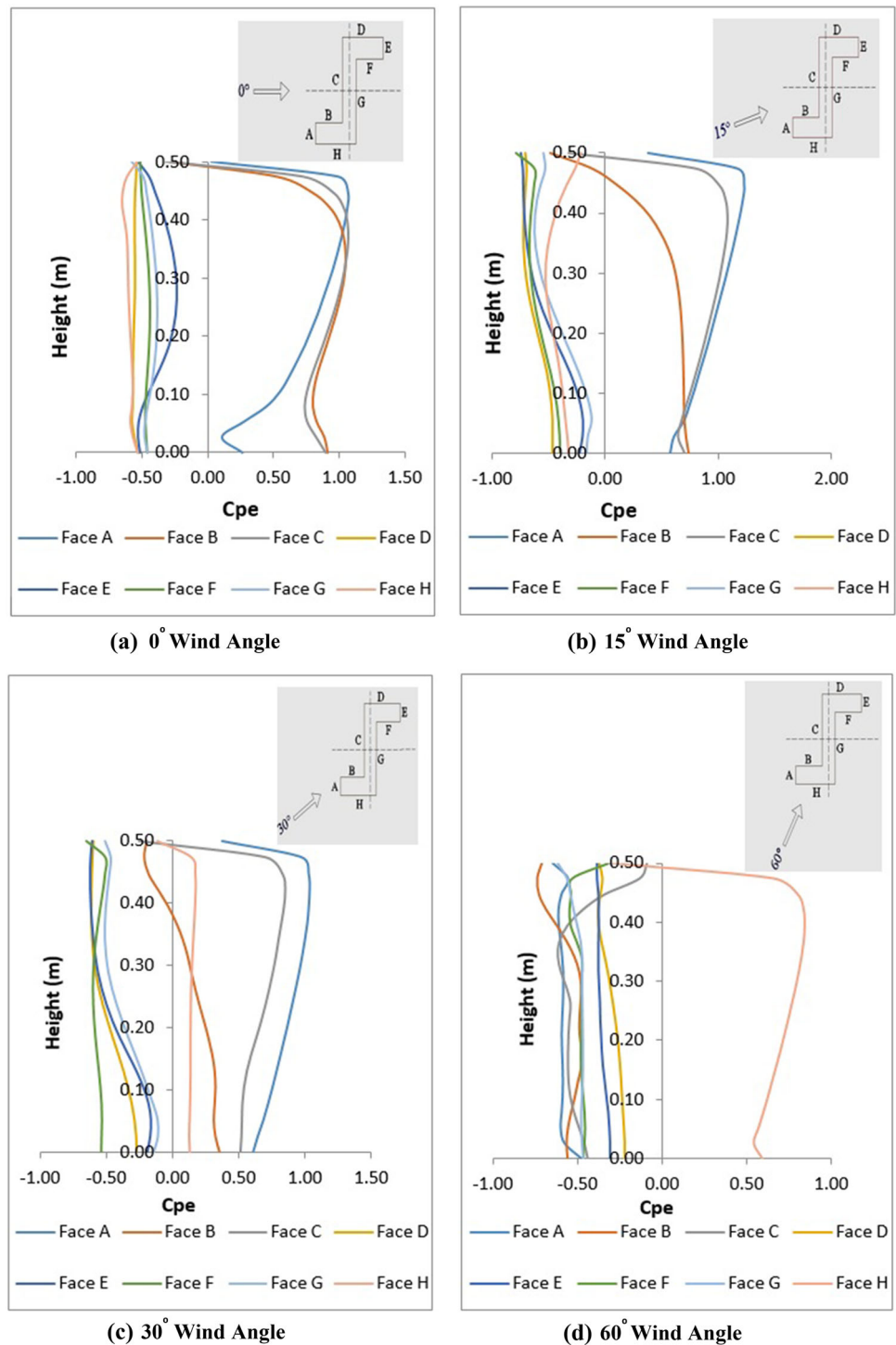
deviation of pressure is wide for Face E. There is non-uniform variation of suction pressure up to a certain height for this face and thereafter the pressure becomes positive. The other faces are under more or less uniform negative pressures.

The variation of wind pressure along the horizontal centerline of all the faces of the building for wind angles 0°, 15°, 30°, 60°, 90°, 120° and 150° are shown in Figs. 15, 16, 17, 18, 19, 20 and 21 respectively. Three different heights of the building are considered to take into account

Fig. 14 continued

(e) 90° Wind Angle

(f) 120° Wind Angle

(g) 150° Wind Angle
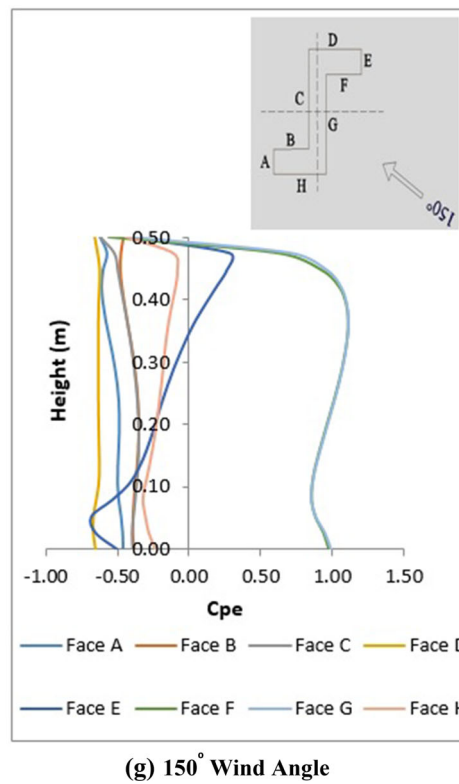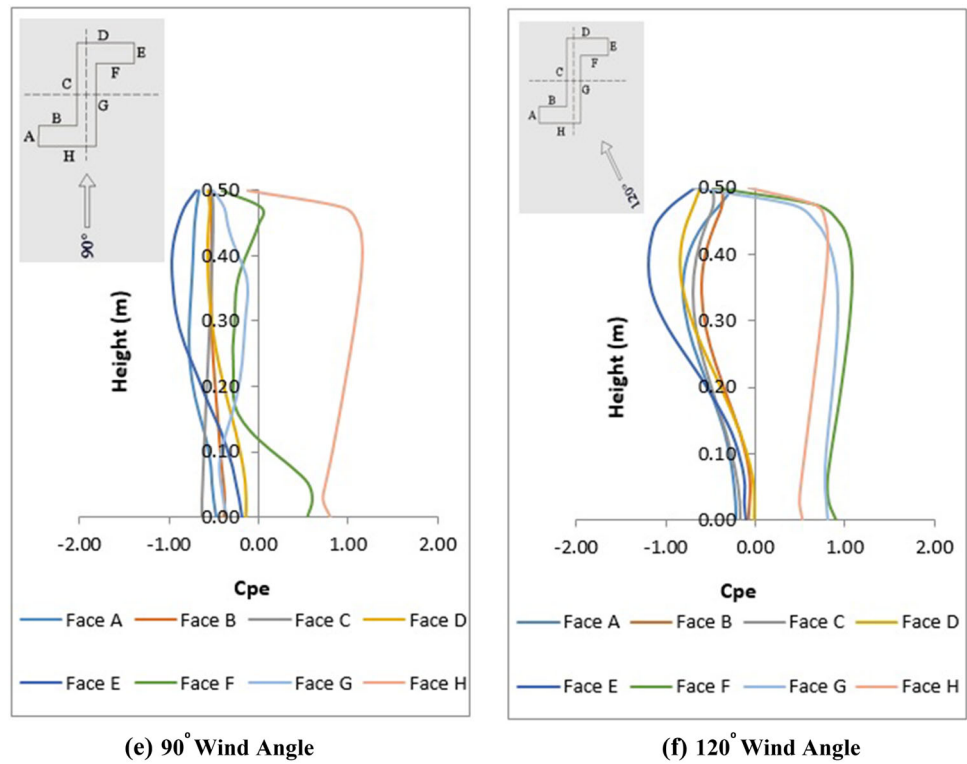
the variation along the height as well. The ordinate of the graph is the external pressure coefficient (C_{pe}) of each face and along the abscissa the perimeter of the building is plotted. These plots support understanding the overall scenario, i.e., the response of all the faces of the building under a particular wind incidence angle. For 15° wind

Fig. 15 Comparison of pressure coefficients along the horizontal line through various faces at three different heights of the building for 0° wind angle
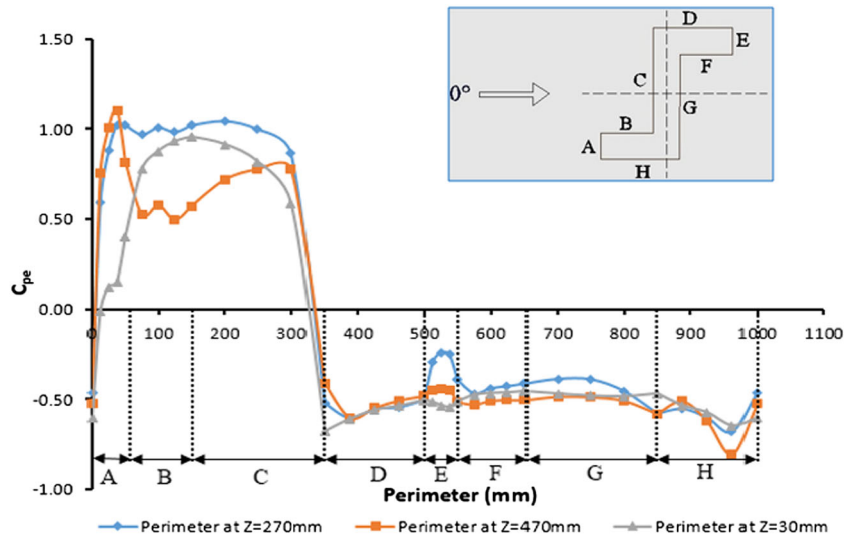
Fig. 16 Comparison of pressure coefficients along the horizontal line through various faces at three different heights of the building for 15° wind angle
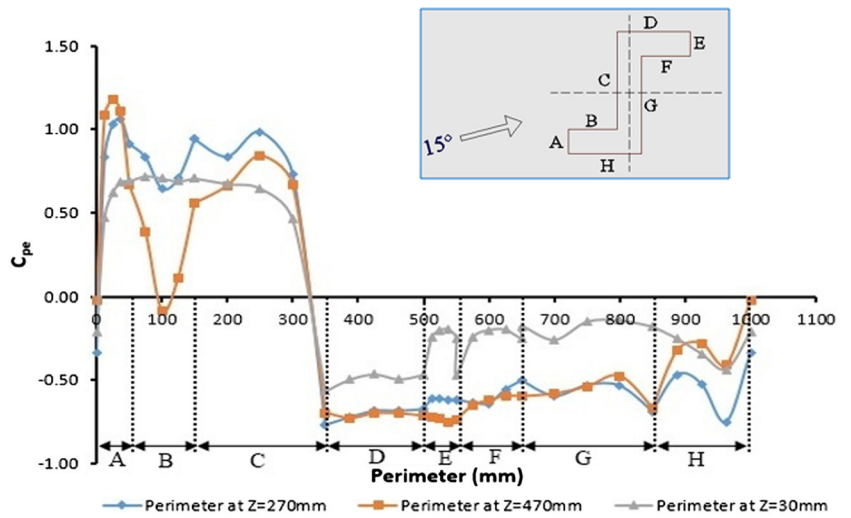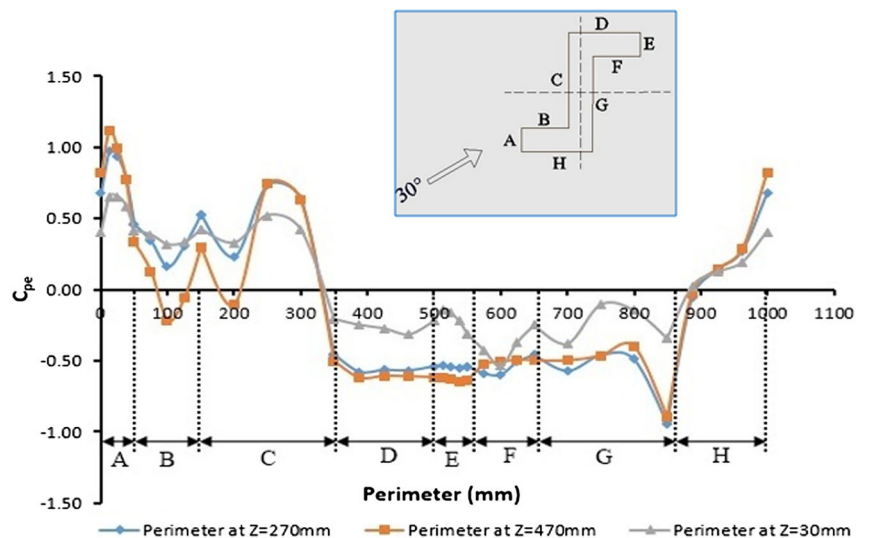

Fig. 17 Comparison of pressure coefficients along the horizontal line through various faces at three different heights of the building for 30° wind angle

Fig. 18 Comparison of pressure coefficients along the horizontal line through various faces at three different heights of the building for 60° wind angle
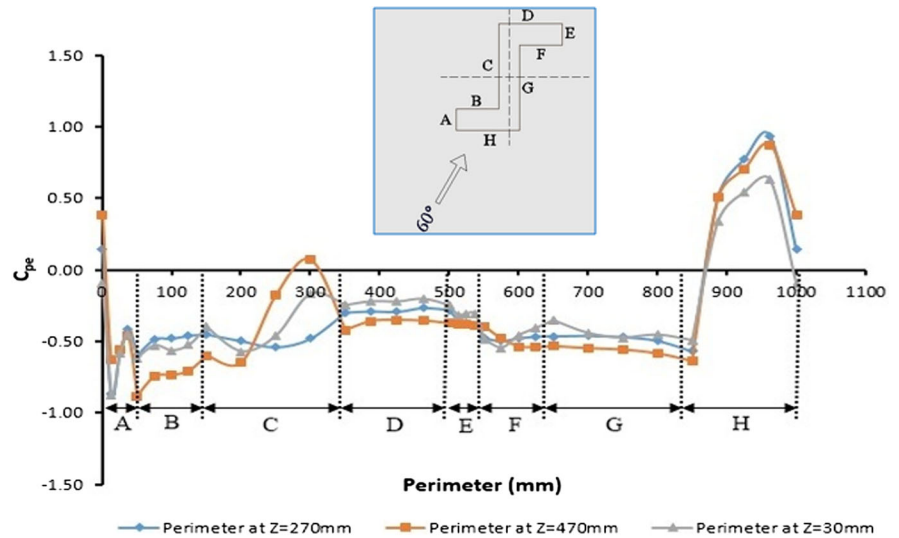

Fig. 19 Comparison of pressure coefficients along the horizontal line through various faces at three different heights of the building for 90° wind angle
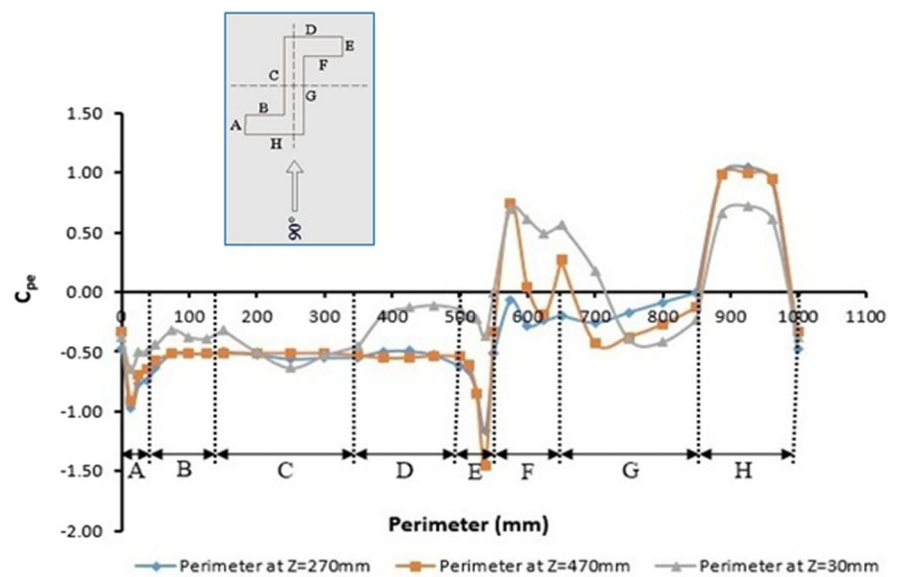

Fig. 20 Comparison of pressure coefficients along the horizontal line through various faces at three different heights of the building for 120° wind angle
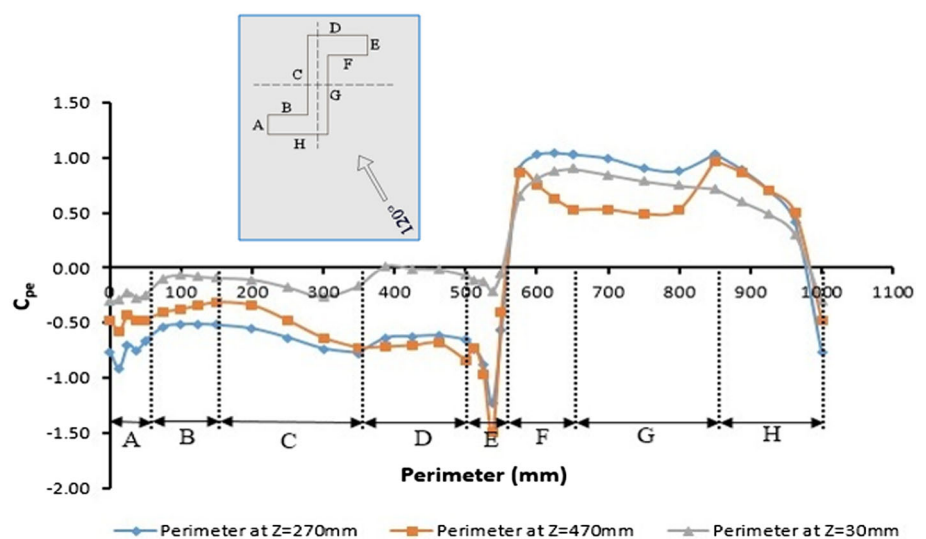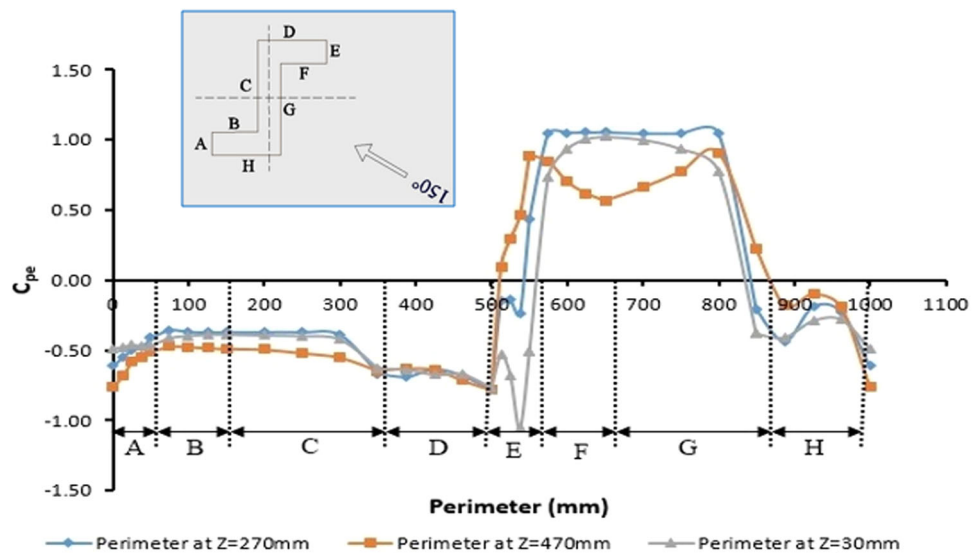
Fig. 21 Comparison of pressure coefficients along the horizontal line through various faces at three different heights of the building for 150° wind angle

angle, even though C_{pe} is positive for Face A, Face B and Face C, there is a sudden fall in C_{pe} at Face B for the height of 470 mm. It touches suction pressure and then rapidly becomes positive again. This may be a result of uplift force at a greater height of the building. For 30°, the nature of variation is more or less similar. The C_{pe} values changes with height only. From the plots, the backwash effects at the lower portion of the building and uplift at greater height are quite clear.

Conclusion

Provisions of the codes are usually available for orthogonal wind directions only. But the results of the study clearly indicate that for tall buildings, a deeper perception of the phenomenon of wind structure interface is needed for more precise information. For that, model analysis is inevitable. The force coefficient (C_f) along the X direction has a maximum value of 1.02 for 15° wind angle and the same along Y is extreme for the 60° wind angle of attack with a value of C_f equal to 1.24. Quite obviously, the windward faces are subjected to positive pressure coefficients because of the undeviating wind force. Because of frictional flow separation and generation of vortices, the leeward faces are exposed to suction. Flow separation characteristics and vortices are quite apparent from the streamlines. The pressure force on the windward side and suction force on the leeward side in combination produce vortices in the wake region, causing the deflection of the body. There may be occurrence of suction even on the windward faces because of the separation of flow in structures with limbs and also due to uplift, sidewash and backwash of wind.

References

Amin JA, Ahuja AK (2013) Effects of side ratio on wind-induced pressure distribution on rectangular buildings. Hindawi Publishing Corporation, J Struct 2013 (**Article ID 176739, 12 pages**)

Bhatnagar NK, Gupta PK, Ahuja AK (2012) Wind pressure distribution on low–rise building with saw-tooth roof. In: IV National Conference on Wind Engineering

Bhattacharyya B, Dalui SK, Ahuja AK (2014) Wind induced pressure on 'E' plan shaped tall buildings. Jordon J Civil Eng 8(2):120–134

Chakraborty S, Dalui SK, Ahuja AK (2014) Wind load on irregular plan shaped tall building—a case study. Wind Struct 18(6):59–73

Fu JY, Li QS, Wu JR, Xiao YQ, Song LL (2008) Field measurements of boundary layer wind characteristics and wind-induced responses of super-tall buildings. J Wind Eng Ind Aerodyn 96(8–9):1332–1358

Gomes M, Rodrigues A, Mendes P (2005) Experimental and numerical study of wind pressures on irregular-plan shapes. J Wind Eng Ind Aerodyn 93:741–756

Irwin A (2007) Bluff body aerodynamics in wind engineering. J Wind Eng Ind Aerodyn 96(6–7):701–712

Irwin A (2009) Wind engineering challenges of the new generation of super-tall buildings. J Wind Eng Ind Aerodyn 97(7–8):328–334

I.S: 875 (Part-3) (1987) Code of practice for the design loads (other than earthquake) for buildings and structures (part-3, wind loads). Bureau of Indian Standards, New Delhi

Kareem A (1986) The effect of Aerodynamic interference on the dynamic response of prismatic structures. J Wind Eng Ind Aerodyn 25(1987):365–372

Kheyari P, Dalui SK (2015) Estimation of wind load on a tall building under interference effects: a case study. Jordon J Civil Eng 9(1):84–101

Kushal T, Ahuja AK, Chakrabarti A (2013) An experimental investigation of wind pressure developed in tall buildings for different plan shape. Int J Innov Res Studies 1(12):605–614

Lam KM, Zhao JG (2006) Interference effects of wind loads on a row of tall buildings. In: The Fourth International Symposium on Computational Wind Engineering (CWE2006), Yokohama

Liang S, Li QS, Lui S, Zhang L, Gu M (2004) Torsional dynamic wind loads on rectangular tall buildings. Eng Struct 26(2004):129–137

Lin N, Letchford C, Tamura Y, Liang B (2004) Characteristics of wind forces acting on tall buildings. J Wind Eng Ind Aerodyn 93(3):217–242

Muehleisen RT, Patrizi S (2013) A new parametric equations for the wind pressure coefficient for low-rise buildings. Energy Build 57(2013):245–249

Raj R, Ahuja AK (2013) Wind loads on cross shape tall buildings. J Acad Ind Res (JAIR) 2(2):111

Revuz J, Hargreaves DM, Owen JS (2012) On the domain size for the steady-state CFD modelling of a tall building. Wind Struct 15(4):313–329

Tominaga Y, Stathopoulos T (2012) CFD modelling of pollution dispersion in building array: evaluation of turbulent scalar flux modelling in RANS model using LES results. J Wind Eng Ind Aerodyn 104–106(2012):484–491

Tse KT, Hitchcock PA, Kwok KCS, Thepmongkorn S, Chan CM (2009) Economic perspectives of aerodynamic treatments of square tall buildings. J Wind Eng Ind Aerodyn 97(9):455–467

Verma SK, Ahuja AK, Pandey AD (2013) Effects of wind incidence angle on wind pressure distribution on square pan tall buildings. J Acad Ind Res 1(12):747–752

Zhang A, Gu M (2008) Wind tunnel tests and numerical simulations of wind pressures on buildings in staggered arrangement. J Wind Eng Ind Aerodyn 96(2008):2067–2079